

Comparative Analysis of Existing Models on Pull-out Stiffness of Glued-in Rod in Glulam

Gwang-Ryul Lee¹, Jaewon Oh², Kyung-Sun Ahn³, Min-Jeong Kim⁴, Sang-Hyun You⁵, Sung-Jun Pang⁶, Chul-ki Kim⁷, Keon-ho Kim⁸, Jung-Kwon Oh⁹

ABSTRACT: This paper presents a comparative analysis of various prediction models for pull-out stiffness in single glued-in rod connections. While extensive research has focused on strength properties, this study specifically addresses the less-explored area of connection stiffness. The study evaluates five existing models for predicting glued-in rod stiffness in glulam. These include three empirical equations and two analytical models. Both analytical models are derived from Volkersen's theory, with one incorporating Timoshenko beam principles and the other excluding them. The predicted values were validated against experimental data originally collected by Oh et al [16], utilizing Japanese larch glulam specimens with various geometric configurations, including different rod diameters (16, 19, and 24 mm), anchorage lengths (200, 300, and 400 mm), and non-bonded lengths (0 and 80 mm). Furthermore, the models were evaluated against experimental data from previous studies [16]-[18]. Results revealed that the model integrating both Volkersen's theory and Timoshenko beam principles exhibited exceptional agreement between theoretical predictions and experimental measurements, with test-to-model ratios ranging from 0.94 to 1.19. Statistical analysis confirmed that this model's accuracy remained consistent across various geometric configurations. This comparative study demonstrates that for reliable prediction of glued-in rod stiffness, both the interaction between timber, rod, and adhesive, as well as the shear deformation of the adherend, must be appropriately considered.

KEYWORDS: Glued-in Rod, Pull-out Stiffness, Timber Connections, Experimental Validation, Adhesive Joints

¹ Gwang-Ryul Lee, dept. of Agriculture, Forestry and Bioresources, Seoul National University, Seoul, Republic of Korea, qweqweqwer@snu.ac.kr

² Jaewon Oh, dept. of Wood Science, University of British Columbia, Vancouver, Canada, jwoh@student.ubc.ca

³ Kyung-Sun Ahn, dept. of Agriculture, Forestry and Bioresources, Seoul National University, Seoul, Republic of Korea, rudtjs6339@snu.ac.kr

⁴ Min-Jeong Kim, dept. of Agriculture, Forestry and Bioresources, Seoul National University, Seoul, Republic of Korea, minjeong.kim@snu.ac.kr

⁵ Sang-Hyun You, dept. of Agriculture, Forestry and Bioresources, Seoul National University, Seoul, Republic of Korea, tkdus2716@snu.ac.kr

⁶ Sung-Jun Pang, dept of Wood Science and Engineering, Chonnam National University, Gwangju, Republic of Korea, email address or ORCID

⁷ Chul-ki Kim, Wood Engineering Division, National Institute of Forest Science, Seoul, Republic of Korea, email address or ORCID

⁸ Keon-ho Kim, Wood Industry Division, National Institute of Forest Science, Seoul, Republic of Korea, email address or ORCID

⁹ Jung-Kwon Oh, dept. of Agriculture, Forestry and Bioresources, Seoul National University, Seoul, Republic of Korea, email address or ORCID

1 – INTRODUCTION

The evolution of mass timber construction has highlighted the critical role of connection systems in structural performance. Dowel-type fasteners like nails, screws and bolts are primarily utilized as traditional connection methods. However, these types of connections often present limitations in not only aesthetic characteristics, but characteristics related with load-bearing capacity. Screws suffer tightening-stresses when predrilled holes are not sufficiently prepared [1], bolted connections show some drawbacks such as initial slippage, limited ductility and energy dissipation capacity [2], [3]. Moreover, from a structural perspective, traditional fasteners are typically considered as pin connections, meaning they have limited capacity to prevent rotation of structural members. These constraints often compel practitioner to introduce supplementary lateral force-resisting elements such as shear walls that compromise architectural flexibility.

In response to these limitations, Glued-in rod (GiR) connections have emerged as an innovative solution, offering several advantages over traditional methods [4]:

- Superior load-bearing capacity parallel to rod
- High rigidity for moment-resisting applications
- Concealed steel components

: Improved fire resistance, corrosion protection, aesthetic

Despite many advantages, the loading mechanism of GiRs is highly complex to explain due to its intrinsic characteristic: interaction of three or more materials. Extensive research has been conducted to comprehend the structural behaviour of GiRs [5]-[15]. These studies expanded our understanding of GiRs, demonstrating that its performance is affected by various parameters like rod diameter, anchorage length, adhesive types/thickness, density of wood and loading conditions. However many studies mainly focus on pull-out strength and failure modes rather than pull-out stiffness. Prediction of connection stiffness remains insufficiently addressed. This gap in understanding hinders the broader implementation of GiR systems in structural applications.

The results presented in this paper were determined as part of an ongoing research project following the theoretical model development by Oh et al. [16]. The primary objective of this investigation is to conduct a comprehensive comparative analysis of the newly developed prediction model against existing models for GiR pull-out stiffness, using experimental data obtained in the previous study [16]-[18]. This comparative approach aims to identify the most reliable prediction methodology and enhance our understanding of the factors influencing GiR stiffness.

2 – BACKGROUND

The analysis of GiR stiffness has multiple methodological challenges. The inherent complexity arises primarily from the composite nature of this connection, which incorporates diverse materials with distinct mechanical properties, making the characterization of stress distribution mechanisms particularly intricate. Additionally, the definition of deformation varies

depending on the type of application of the GiR system. This variability has resulted in a lack of global consensus regarding the fundamental definition of GiR stiffness.

Despite these constraints, various investigations have proposed design equations for quantifying GiR stiffness. The pre-version of Eurocode 1995-2 [19] presented an empirically-derived equation (1) that incorporated fundamental parameters such as material density and rod diameter.

$$K_{GiR} = \frac{\rho^{1.5}d^{1.8}}{40} \quad (1)$$

Similar form of equation is suggested in [20]. Regression equation (2) was derived from GiR tests conducted on various specimens with different densities, rod diameters and anchorage lengths.

$$K_{GiR} = 310 d^{1.55} \rho^{0.34} \quad (2)$$

While these approaches provide simplified method to predict the stiffness of GiRs, they demonstrates notable limitations, particularly in its omission of critical variables including anchorage length.

Another GiR stiffness model considering geometry factors and material property can be found in the prEN 1995-1-1 [21]. This model include the effect of rod bonded length unlike (1), (2).

$$K_{GiR} = 2 d^{0.6} L^{0.6} \rho^{0.9} \quad (3)$$

However, the model provides insufficient insight into the underlying mechanical behavior of the system, the interaction among timber, adhesive and rod. A more sophisticated approach (4) founded upon Volkersen's theory was developed by Jensen et al. [22] and validated by Ling et al. [23].

$$K_{GiR} = \pi d L \Gamma \frac{(1+\alpha) \sinh \bar{\omega}}{\omega(1+\alpha \cosh \bar{\omega})} \quad (4)$$

This methodology offers a more comprehensive representation of GiR behavior by accounting for the non-uniform distribution of shear stress along the adhesive line, with stress concentrations at the terminal regions. However, this approach exhibits significant limitations as it does not reflect the deformation through shear and bending action of adherends specifically in regions of surrounding timber. Given timber's low shear stiffness, exclusion of these deformations can result in substantial overestimation of system stiffness.

Equation (5), which is derived from the solution of governing differential equations, was proposed by Hassanieh et al. [24] enabling a more detailed analysis of stress distribution patterns.

$$K_{GiR} = P \left(\frac{\frac{D E_c v_r d^2}{A_c} + \frac{v_r d^2}{2 E_r w_1 w_2}}{2 E_r w_1 w_2} (C_1 w_2 (e^{w_1 L} - 1) + C_2 w_2 (1 - e^{w_1 L}) + C_3 w_1 (e^{w_2 L} - 1) + C_4 w_1 (1 - e^{w_2 L})) \right)^{-1} \quad (5)$$

While this approach demonstrates good accuracy, its application is constrained by the requirement for complex numerical methods and computational procedures, rendering it less suitable for practical applications.

Recently, a theoretical model of pull-out stiffness of GiR was developed [16], incorporating Volkersen's theory and Timoshenko beam theory. This model balances between equation's simplicity and accuracy, considering the general geometry and materials properties of GiR systems.

$$K_{GiR} = \frac{E_r A_r}{L} \left(\frac{1}{2} + \mu \frac{d^{1.5}}{L} \right)^{-1} \quad (6)$$

$$\mu = \sqrt{\frac{G_a}{t_a} \frac{8E_r}{G_t^2} \frac{(\sqrt{\alpha+1}-1)(2\sqrt{\alpha+1}+1)}{24(\sqrt{\alpha+1}+1)^2}} \quad (7)$$

According to this model, non-bonded length of GiRs can be thought of as an extension of the rod. So the tensile deformation of rod should be added to the total deformation of GiR.

$$K_{GiR,nb} = \frac{E_r A_r}{L} \left(\frac{1}{2} + \mu \frac{d^{1.5}}{L} + \frac{L}{L_{nb}} \right)^{-1} \quad (8)$$

Although, the authors mentioned that there still remains some limitations, e.g., the effect of other parameters such as grain direction, knots and type of rods were not reflected, the model showed good agreement with experimental stiffness.

3 – Materials and Method

The experimental methodology and data utilized in this comparative study were originally implemented and collected by Oh et al. [16] as part of their development of a novel theoretical model for pull-out stiffness. This section provides a summary of those experimental procedures for completeness and context.

3.1 Specimen Design and Configuration

The experimental investigation utilized specimens made of Japanese larch (*Larix kaempferi*) glued-laminated timber (GLT). The rods were inserted into each side of the GLT to test specimens under practical loading conditions, i.e., pull-pull condition. The detailed geometry and sizes are illustrated in Figure 1.

3.2 Materials

The GLT specimens were manufactured under controlled conditions with moisture content maintained below 12%.

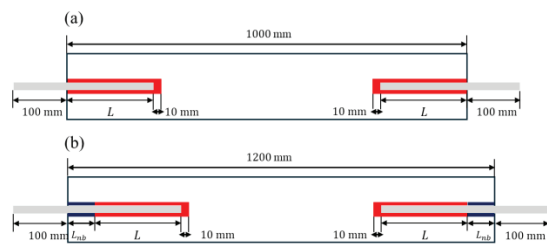


Figure 1. Detailed specimen configurations (a) fully-bonded (b) partially-bonded.

The average air-dried density was 560.7 kg/m³. Material properties were established according to standardized specifications [25] as shown in Table 1, rather than individual testing to ensure consistency with practical applications.

3.2.2 Adhesive

A two-component epoxy adhesive (HIT-RE 500 V3) was selected for its superior bonding characteristics with both steel and wood. The adhesive properties are demonstrated in Table 2, which can be found in the manufacturer's technical data sheet [26].

3.2.3 Steel Rods

Threaded rods classified as grade SS275 according to KS D 3503 [27] were utilized, offering the following advantages: enhanced bond strength through increased surface area and facilitation of rapid assembly through nut connections. The material properties are listed in Table 3.

Table 1. Material properties of Japanese Larch.

Property	Value(Mpa)
Bending strength (characteristic)	10
Modulus of elasticity (average)	9000

Table 2. Material properties of HIT-RE 500 V3.

Property (after 7 days)	Value(Mpa)
Tensile strength (average)	49.3
Compressive strength (average)	82.7
Modulus of elasticity (average)	2600

Table 3. Material properties of SS275.

Property	Value(Mpa)
Tensile yield strength (average)	275
Tensile ultimate strength (average)	400
Modulus of elasticity (average)	210,000

Figure 2. Manufacture process of glued-in rod of (a) external fixation equipment (b) partially non-bonded specimen



3.3 Specimen preparation

The specimen preparation process involved careful consideration of manufacturing precision and quality control measures. Key aspects included:

- Drilling holes with diameters 2-3 mm larger than the rod diameter
- Drilling holes 10mm longer than anchorage length
- Careful adhesive application procedures to prevent air pocket formation
- Use of external fixation equipment or plastic tubes for rod centering as shown in Figure 2. *Manufacture process of glued-in rod of (a) external fixation equipment (b) partially non-bonded specimen.*

Before rod insertion, epoxy adhesives were injected into the drilled hole. In the case of GiR with nonbonded region, plastic tube and rod were inserted before injection of adhesive to hold the rod in the center of hole. Therefore, it was not able to inject adhesive directly through the hole. To address this issue, pre-holes on the side of timber were drilled as illustrated in Figure 2. *Manufacture process of glued-in rod of (a) external fixation equipment (b) partially non-bonded specimen* (b), and adhesive was injected until it flowed through the other pre-hole.

The specimens were designed to evaluate the influence of geometric parameters on GiR pull-out stiffness. The primary variables investigated included:

- Rod diameters: 16, 19 and 24 mm
- Anchorage lengths: 200, 300 and 400 mm
- Non-bonded lengths: 0 and 80 mm

The detailed dimensions of GiR specimens are established in Table 4. For each specimen configuration, 3 samples were fabricated.

The GiR specimens were manufactured by GLT graded as 10S-30B according to KS F 3021 [25]. The cross-sectional dimensions were 150 × 150 mm to ensure compliance with minimum edge distance requirements [28].

3.4 Testing configuration and method

The experimental investigation employed a comprehensive testing setup designed to accurately measure pull-out stiffness under controlled conditions. The 1000 kN capacity load cell was used for the test and was combined with protruded rod through nuts as demonstrated in Figure 3. In preliminary tests using only one nut per rod, failures relevant to the nut occurred. To prevent unintended failure modes, double nuts were adopted for the test.

Table 4. Detailed dimensions of specimens

Specimen Name	d_r	t_a	L	L_{nb}
16-200	16	2	200	0
16-300			300	0
16-400			400	0
19-200	19	3	200	0
19-300			300	0
19-400			400	0
24-300	24	3	300	0

24-400			400	0
16-200-nb	16	2	200	80
16-300-nb			300	80
16-400-nb			400	80

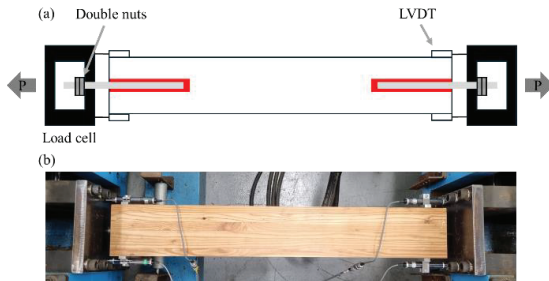


Figure 3 Testing configuration (a) schematic representation (b) actual setup configuration.

Linear variable displacement transducers (LVDTs) were installed on both sides of the specimens. LVDTs were positioned at the timber ends to measure relative displacement of the rods and wood. For each rod, two LVDTs were allocated to minimize error caused by unintended movement of the specimen, such as rotation of specimen due to the tolerance of the drilled hole in load cell.

One side of specimen was fixed not to move, and forces were applied through another side of rod with loading rate of 2mm/min. Loads were imposed until a significant drop occurred or representative failure modes of GiR were observed, such as pull-out of the wood block, splitting of the wood, or tensile failure of the rod.

4 RESULTS

4.1 Experimental Results

The load-displacement curves of pull-out tests are shown in Figure 4, categorized according to rod diameter and anchorage length. Individual test results are depicted in gray, with averaged curves represented by red lines. Initial linear elastic behaviors are observed across all GiR configurations. After the elastic region, strain-softening behavior was observed due to yielding of rods. Loads exceeding the design yield load of rods were applied for all specimens. As the anchorage length to rod diameter ratio increases, strain-softening effect becomes distinct.

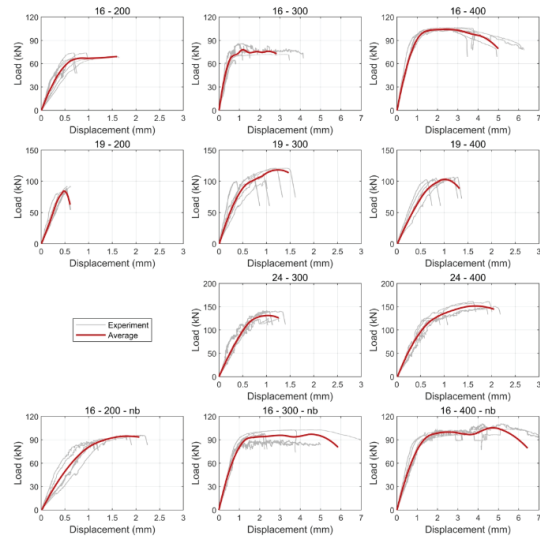


Figure 4. Experimental load-displacement curves of GiRs.

Table 5 presents pull-out stiffness values of experiments (K_{test}). The assessment of pull-out stiffness was based on

Table 5. Stiffness of GiR(test data).

Specimen Name	K_{test} (kN/mm)	COV (%)
16-200	145.25	35.41
16-300	130.42	14.01
16-400	115.83	3.78
19-200	175.40	15.24
19-300	190.65	13.52
19-400	151.80	13.89
24-300	228.74	23.77
24-400	198.44	13.17
16-200-nb	103.67	35.94
16-300-nb	103.51	13.63
16-400-nb	81.83	17.15

average relative deformation data measured by LVDTs at the glued-laminated timber (GLT) end face as demonstrated in Figure 3. To accurately evaluate displacement of the GiR, the tensile deformation of the protruding rod was subtracted from observed displacement values. This deformation was calculated assuming an axial stiffness of EA/L for the protruding rod section. Pull-out stiffness values were determined through linear regression analysis of the initial elastic region.

The maximum displacements during the linear region were less than 1mm in all specimens, which means that experimental measurements were very sensitive to potential errors. To enhance analytical robustness, data points deviating by more than three standard deviations from mean values were classified as outliers and excluded from subsequent analysis. Despite diligent experimental set-up, it should be noted that the test error could not be eliminated perfectly. Even minor rotational movement during pull-out testing can introduce significant

deformation errors, potentially resulting in stiffness value deviations remarkably (e.g., approximately 0.01 rad induces 0.05 mm displacement errors and it affects the stiffness more than 10%). This underscores the necessity for enhanced deformation measurement methodologies in future investigations.

Table 5 shows the influence of geometric factors on the stiffness of GiR. Experimental results demonstrate a positive correlation between pull-out stiffness and rod diameter. This trend can be attributed to enhanced stress dispersion across expanded bonding regions, resulting in reduced deformation and increased stiffness. Conversely, in this research, as the anchorage length increases, the stiffness of specimen tends to decrease slightly—although previous studies [9], [17], [24] reported no direct correlation between these two parameters—which can be explained by (6) and (8).

Table 6. Prediction of GiRs stiffness with existing models and ratio of test stiffness values to model prediction values.

Specimen Name	GiR Stiffness Models									
	Model 1 [19]		Model 2 [20]		Model 3 [21]		Model 4 [22]		Model 5 [16]	
	K_{model} (kN/mm)	K_{test}/K_{model}	K_{model} (kN/mm)	K_{test}/K_{model}	K_{model} (kN/mm)	K_{test}/K_{model}	K_{model} (kN/mm)	K_{test}/K_{model}	K_{model} (kN/mm)	K_{test}/K_{model}
16-200	48.80	2.98	196.03	0.74	75.51	1.92	769.44	0.19	136.90	1.06
16-300	48.80	2.67	196.03	0.67	96.30	1.35	769.48	0.17	116.98	1.11
16-400	48.80	2.37	196.03	0.59	114.44	1.01	769.48	0.15	102.13	1.13
19-200	66.50	2.64	255.86	0.69	83.71	2.10	812.74	0.22	186.10	0.94
19-300	66.50	2.87	255.86	0.75	106.76	1.79	813.01	0.23	159.87	1.19
19-400	66.50	2.28	255.86	0.59	126.87	1.20	813.02	0.19	140.12	1.08
24-300	101.26	2.26	367.50	0.62	122.83	1.86	1154.17	0.20	205.34	1.11
24-400	101.26	1.96	367.50	0.54	145.97	1.36	1154.22	0.17	184.42	1.08
16-200-nb	-	-	-	-	-	-	-	-	107.59	0.96
16-300-nb	-	-	-	-	-	-	-	-	94.9	1.09
16-400-nb	-	-	-	-	-	-	-	-	84.88	0.96

Specimens with non-bonded regions exhibited decreased pull-out stiffness compared to configurations with equivalent bonded lengths. This reduction likely results from increased rod tensile deformation while timber shear deformation remains constant. Therefore, while non-bonded regions may enhance pull-out strength characteristics, they appear to adversely affect pull-out stiffness performance.

4.2 Comparison of Experimental Results and Theoretical Predictions

Theoretical predictions of pull-out stiffness (K_{model}) were calculated using (1)-(4) and (6) for full-bonded specimens and (8) for partially non-bonded GiRs. The results are summarized in Table 5. Several supplementary assumptions were necessary for these calculations. Since Korean standard specifications do not provide explicit shear modulus (G_t) values for GLT, $E_t/16$ was employed in accordance with Eurocode 5 [19]. Additionally, the shear modulus of the epoxy adhesive was derived assuming a Poisson's ratio of 0.2, following Hassanieh et al. [24].

The empirical model 1 and 3 showed underestimated stiffness of GiRs, while empirical model 2 and theoretical model 4 predicted higher values than experimental values. The theoretical model 5 demonstrated good

agreement with experimental observations with K_{test}/K_{model} values ranging from 0.94 to 1.19. Notably, these variations and the coefficients of variance in experimental data showed no systematic correlation with specific geometric configurations.

To statistically verify the effect of geometric variance, t-tests were performed between specimen configurations. As shown in Table 7, only in model 5, the null hypothesis ($H_0: u_1 = u_2$) was not rejected for all configurations at a significance level of 0.05 (p-value > 0.05, Table 7). This suggests that model 5 prediction accuracy is not affected by rod diameter and anchorage length while other models accuracy were differ as GiR geometry factors change.

Additional validation was conducted through comparative analysis with experimental data from previous studies [17], [18]. Table 8 summarizes the ratio of experimental observations and model calculation values from earlier research. For consistency, the shear modulus of timber and adhesive were assumed as mentioned before.

Table 7. t-test results between specimen configurations.

p-value ($H_0: u_1 = u_2$)		$u_1 (K_{test}/K_{model})$										
		16-200	16-300	16-400	19-200	19-300	19-400	24-300	24-400	16-200-nb	16-300-nb	16-400-nb
$u_2 (K_{test}/K_{model})$	16-200	1.0000	0.8298	0.7544	0.6367	0.6071	0.9284	0.8515	0.9514	0.7578	0.9047	0.7035
	16-300		1.0000	0.8470	0.2321	0.5814	0.8136	0.9961	0.7655	0.5282	0.8556	0.3148
	16-400			1.0000	0.0912	0.5771	0.6040	0.9026	0.5339	0.4449	0.6524	0.1597
	19-200				1.0000	0.1154	0.3060	0.3800	0.3157	0.9272	0.2821	0.8729
	19-300					1.0000	0.4396	0.6833	0.4004	0.3578	0.4664	0.1618
	19-400						1.0000	0.8703	0.9539	0.6119	0.9548	0.4077
	24-300							1.0000	0.8375	0.5823	0.9010	0.4524
	24-400								1.0000	0.6302	0.9073	0.4235
	16-200-nb									1.0000	0.5903	0.9983
	16-300-nb										1.0000	0.3797
	16-400-nb											1.0000

Table 8. Comparison of test and predicted stiffness of GiR in previous studies.

References	Species	Rod type	d_r	t_a	L	t_a	K_{test}/K_{model}				
							Model 1 [19]	Model 2 [20]	Model 3 [21]	Model 4 [22]	Model 5 [16]
[17]	Douglas fir	Steel rebar	16	2	120	2	5.31	1.10	4.25	0.18	1.00
		Steel rebar		2	160	2	5.42	1.13	3.65	0.18	1.12
		Steel rebar		2	200	2	5.59	1.16	3.29	0.19	1.26
		Steel rebar		4	200	4	6.08	1.26	3.58	0.29	1.14
		Steel rebar		6	200	6	5.25	1.09	3.09	0.31	0.90
[18]	Beech	Threaded rod	16	2	160	2	3.50	1.17	3.01	0.19	1.00
		Rebar standard		2	160	2	3.85	1.28	3.30	0.21	1.10
		Rebar inox		2	160	2	3.78	1.26	3.24	0.21	1.08
	Oak	Threaded rod	16	2	160	2	2.54	0.90	2.25	0.15	0.84
		Rebar standard		2	160	2	3.55	1.25	3.13	0.21	1.17
		Rebar inox		2	160	2	3.42	1.20	3.02	0.20	1.13

Among empirical models, model 2 predicted the stiffness of GiRs well, while model 1 and model 3 significantly underestimated the stiffness values. On the other hand, theoretical model 4 overestimated the GiR stiffness. Because model 4 does not incorporate the deformation of timber adherend, it consistently provides a high evaluation of the stiffness of GiR. The theoretical model 5 shows high accuracy in predicting the stiffness characteristics reported in previous studies, though it generally yields more conservative estimations. This systematic underestimation can be attributed to the dimensional discrepancy between nominal and effective diameters in threaded rod configurations—the diameter of threaded rods for (6) and (8) being reduced due to their helical profile, resulting in diminished stiffness properties. This observation corresponds with previously established findings in the literature documenting the stiffness of threaded rod systems [18], [23]. The propensity toward conservative prediction suggests that this model inherently incorporates a safety margin when applied with various types of rod, rendering it particularly suitable for engineering design applications.

5 – CONCLUSION

This comparative study has investigated multiple prediction methodologies for pull-out stiffness of glued-in rod timber connections, including empirical models [19], [20], [21] and theoretical models [16], [22]. Through extensive validation against experimental data, the following conclusions can be derived:

Geometric parameters exhibited significant influence on glued-in rod stiffness. Rod diameter demonstrated a positive correlation with pull-out stiffness, while anchorage length and non-bonded regions substantially diminished stiffness values. The influence of anchorage length proved to be more subtle, with longer anchorage lengths yielding marginally lower stiffness values.

Empirical models generally predicted lower stiffness of GiR than experimental values, while theoretical model derived from Volkersen theory calculated higher values. Among existing models, the analytical model, which is developed through the integration of Volkersen's theory and Timoshenko beam principles, demonstrates remarkable efficacy in predicting GiR pull-out stiffness across diverse geometric configurations. This finding

emphasizes the importance of shear deformations of timber when evaluating the stiffness of GiRs due to relatively low shear stiffness of wood adherend.

The model 5, which most accurately provided the GiRs stiffness, showed a tendency toward slightly conservative estimation. This propensity might be induced by the configuration of rod, that effective diameter would be larger than nominal value. Variation tendency in K_{test}/K_{model} ratios from geometric difference was not found according to t-test results which means that this theoretical model can predict the stiffness of GiR regardless of GiR geometric factors.

However, further research is needed to extend our knowledge of GiR behavior, e.g., the influence of adhesive thickness, timber density, and alternative rod configurations. Furthermore, endeavors to refine testing methods to mitigate the unintended displacement such as specimen rotation are needed to more exactly examine the stiffness values.

The findings from this study contribute meaningfully to our understanding of GiR systems and provide engineering practitioners which mechanisms should be considered for GiR design applications. This research might potentially facilitate broader implementation of these innovative connection solutions in contemporary timber structures.

6 – Nomenclature

K_{GiR} : Pull-out stiffness of GiR(kN/mm)

ρ : Density of timber (kg/m³)

d : Rod diameter (mm)

L : Anchorage length (mm)

L_{nb} : Non-bonded length (mm)

Γ : Shear stiffness factor of adhesive

α : Ratio of axial stiffness of timber to rod

$\bar{\omega}$: Coefficient of brittleness ratio

A_c, D_c, w_i, C_i : Coefficients

E_r, E_w : Modulus of elasticity of rod and wood (MPa)

A_r, A_w : Cross-section area of rod and wood(mm²)

G_a : Shear stiffness of adhesive (MPa)

t_a : thickness of adhesive (mm)

7 – REFERENCES

- [1] H. W. Lee, S. S. Jang, and C.-W. Kang, "Evaluation of Withdrawal Resistance of Screw-Type Fasteners Depending on Lead-Hole Size, Grain Direction, Screw Size, Screw Type and Species," *Journal of the Korean Wood Science and Technology*, vol. 49, no. 2, pp. 181–190, Mar. 2021, doi: 10.5658/WOOD.2021.49.2.181.
- [2] N. Gattesco and I. Toffolo, "Experimental study on multiple-bolt steel-to-timber tension joints," *Mat. Struct.*, vol. 37, no. 2, pp. 129–138, Mar. 2004, doi: 10.1007/BF02486609.
- [3] Z. Shu *et al.*, "Reinforced moment-resisting glulam bolted connection with coupled long steel rod with screwheads for modern timber frame structures," *Earthquake Engineering & Structural Dynamics*, vol. 52, no. 4, pp. 845–864, 2023, doi: 10.1002/eqe.3789.
- [4] G. Tlustochowicz, E. Serrano, and R. Steiger, "State-of-the-art review on timber connections with glued-in steel rods," *Mater Struct*, vol. 44, no. 5, pp. 997–1020, Jun. 2011, doi: 10.1617/s11527-010-9682-9.
- [5] S. Aicher and H.-W. Reinhardt, *PRO 22: International RILEM Symposium on Joints in Timber Structures*. RILEM Publications, 2001.
- [6] J. G. Broughton and A. R. Hutchinson, "Pull-out behaviour of steel rods bonded into timber," *Materials and Structures*, vol. 34, 2001.
- [7] R. Steiger, E. Gehri, and R. Widmann, "Pull-out strength of axially loaded steel rods bonded in glulam parallel to the grain," *Mater Struct*, vol. 40, no. 1, pp. 69–78, Jan. 2007, doi: 10.1617/s11527-006-9111-2.
- [8] J. Estévez Cimadevila, J. A. Vázquez Rodríguez, and M. D. Otero Chans, "Experimental behaviour of threaded steel rods glued into high-density hardwood," *International Journal of Adhesion and Adhesives*, vol. 27, no. 2, pp. 136–144, Mar. 2007, doi: 10.1016/j.ijadhadh.2006.01.006.
- [9] B. Azinović, E. Serrano, M. Kramar, and T. Pazlar, "Experimental investigation of the axial strength of glued-in rods in cross laminated timber," *Mater Struct*, vol. 51, no. 6, p. 143, Oct. 2018, doi: 10.1617/s11527-018-1268-y.
- [10] E. Toumpanaki and M. H. Ramage, "Glued-in CFRP and GFRP rods in block laminated timber subjected to monotonic and cyclic loading," *Composite Structures*, vol. 272, p. 114201, Sep. 2021, doi: 10.1016/j.compstruct.2021.114201.
- [11] S. Navaratnam, J. Thamboo, T. Ponnampalam, S. Venkatesan, and K. B. Chong, "Mechanical

- performance of glued-in rod glulam beam to column moment connection: An experimental study,” *Journal of Building Engineering*, vol. 50, p. 104131, Jun. 2022, doi: 10.1016/j.jobe.2022.104131.
- [12] P. J. Gustafsson and E. Serrano, “Glued-In Rods for Timber Structures - Development of a Calculation Model,” *Division of Structural Mechanics, LTH*, 2001.
- [13] E. Serrano and P. J. Gustafsson, “Fracture mechanics in timber engineering – Strength analyses of components and joints,” *Mater Struct*, vol. 40, no. 1, pp. 87–96, Jan. 2007, doi: 10.1617/s11527-006-9121-0.
- [14] D. Otero Chans, J. E. Cimadevila, and E. M. Gutiérrez, “Model for predicting the axial strength of joints made with glued-in rods in sawn timber,” *Construction and Building Materials*, vol. 24, no. 9, pp. 1773–1778, Sep. 2010, doi: 10.1016/j.conbuildmat.2010.02.010.
- [15] A. Rossignon and B. Espion, “Experimental assessment of the pull-out strength of single rods bonded in glulam parallel to the grain,” *Holz Roh Werkst*, vol. 66, no. 6, pp. 419–432, Dec. 2008, doi: 10.1007/s00107-008-0263-3.
- [16] J. Oh *et al.*, “Theoretical modeling of pull-out stiffness of glued-in single rod in timber,” *Engineering Structures*, vol. 325, p. 119346, Feb. 2025, doi: 10.1016/j.engstruct.2024.119346.
- [17] Z. Ling, H. Yang, W. Liu, W. Lu, D. Zhou, and L. Wang, “Pull-out strength and bond behaviour of axially loaded rebar glued-in glulam,” *Construction and Building Materials*, vol. 65, pp. 440–449, Aug. 2014, doi: 10.1016/j.conbuildmat.2014.05.008.
- [18] C. Grunwald *et al.*, “Rods glued in engineered hardwood products part I: Experimental results under quasi-static loading,” *International Journal of Adhesion and Adhesives*, vol. 90, pp. 163–181, Apr. 2019, doi: 10.1016/j.ijadhadh.2018.05.003.
- [19] European Committee for Standardization, *prEN 1995-2 Design of timber structures, Part 2: Bridges*. Brussels, Belgium: Final Project Team draft. Stage 34, 2003.
- [20] C. Binck and A. Frangi, “On stiffness and strength of glued-in rods and threaded rods parallel to the grain,” 2024, doi: 10.3929/ETHZ-B-000720943.
- [21] European Committee for Standardization, *prEN 1995-1-1 Design of timber structures, Part 1-1: General Common rules and rules for buildings*. Brussels, Belgium, 2023.
- [22] J. L. Jensen, A. Koizumi, T. Sasaki, Y. Tamura, and Y. Iijima, “Axially loaded glued-in hardwood dowels,” *Wood Science and Technology*, vol. 35, no. 1, pp. 73–83, Apr. 2001, doi: 10.1007/s002260000076.
- [23] Z. Ling, W. Liu, H. Yang, and X. Chen, “Modelling of glued laminated timber joints with glued-in rod considering bond-slip location function,” *Engineering Structures*, vol. 176, pp. 90–102, Dec. 2018, doi: 10.1016/j.engstruct.2018.08.098.
- [24] A. Hassanieh, H. R. Valipour, M. A. Bradford, and R. Jockwer, “Glued-in-rod timber joints: analytical model and finite element simulation,” *Mater Struct*, vol. 51, no. 3, p. 61, Jun. 2018, doi: 10.1617/s11527-018-1189-9.
- [25] Korean Standards Association, *KS F 3021: Structural glued laminated timber*. 2013.
- [26] North American Product Technical Guides 22nd ed., *Anchor Fastening Technical Guide*, 2 vols. Hilti Inc., 2022.
- [27] Korean Standards Association, *KS D 3503: Rolled steels for general structure*. 2016.
- [28] EOTA, *Design of Glued-in Rods for Timber Connections*, vol. TR 070. European Organisation for Technical Assessment (EOTA), 2019.